Chitosan-Coated Alginate Nanoparticles for Oral Insulin Delivery: Box-Behnken Optimization, pH-Responsive Release, Enzymatic Protection and In Vitro Permeation

Ayush Kumar Srivastava[1], Ved Prakash Tiwari[2], Ashish Kumar Srivastav[3], Bandana Singh[4]
[1,2,3,4]*Goel Institute of Pharmaceutical Sciences, Lucknow, U.P. India*

***Abstract*—Oral insulin delivery remains limited by acidic gastric conditions, enzymatic degradation, mucus diffusion barriers and low epithelial permeability. This study formulated chitosan-coated calcium alginate nanoparticles as an aqueous, polymeric carrier for improving the in vitro oral delivery potential of insulin. Insulin-loaded nanoparticles were prepared by ionic gelation using sodium alginate, calcium chloride and chitosan. A three-factor, three-level Box-Behnken design evaluated the effects of alginate concentration, chitosan concentration and calcium chloride concentration on particle size, polydispersity index, zeta potential, entrapment efficiency and simulated gastrointestinal release. A desirability-selected formulation containing sodium alginate 1.425 mg/mL, chitosan 0.660 mg/mL and calcium chloride 21.5 mM showed particle size 221.4 ± 3.7 nm, PDI 0.214 ± 0.011, zeta potential +25.7 ± 1.6 mV, entrapment efficiency 78.6 ± 1.2%, drug loading 7.8 ± 0.3% and process yield 74.8 ± 1.5%. The optimized nanoparticles restricted insulin release in simulated gastric fluid to 8.7 ± 0.4% at 2 h and then provided controlled release of 70.3 ± 1.6% at 8 h and 86.1 ± 2.1% at 12 h in intestinal media. Insulin remaining after pepsin exposure in simulated gastric fluid was 88.9 ± 2.4% for nanoparticles compared with 28.6 ± 3.1% for insulin solution. Cumulative permeation at 8 h increased from 19.1 ± 1.4% for insulin solution to 48.6 ± 2.8% for nanoparticles, corresponding to an apparent permeability enhancement of 2.60-fold. These findings support chitosan-coated alginate nanoparticles as a promising in vitro platform for pH-responsive insulin protection and absorption-related enhancement. In vivo pharmacokinetic, pharmacodynamic, safety and insulin-bioactivity studies are required before claims of true oral bioavailability or therapeutic efficacy can be made.**

***Index Terms*—oral insulin; chitosan; sodium alginate; nanoparticles; ionic gelation; Box-Behnken design; pH-responsive release; in vitro permeation.**

I. INTRODUCTION

Insulin therapy is central to the management of type 1 diabetes and is frequently required in advanced type 2 diabetes. Subcutaneous injection is effective, but repeated injections can reduce treatment acceptance and do not fully reproduce portal-hepatic insulin exposure. Oral delivery is therefore attractive because it is non-invasive and may better align with endogenous insulin transport; however, insulin is a hydrophilic peptide with low membrane permeability and high sensitivity to acidic pH, proteases and interface-induced destabilization [1-5].

The gastrointestinal tract presents sequential barriers to insulin: acidic gastric fluid can disrupt structure, pepsin and pancreatic enzymes cleave peptide bonds, mucus can retard diffusion, epithelial tight junctions restrict paracellular transport and absorbed insulin may undergo presystemic handling. Polymeric nanocarriers are widely investigated to overcome these barriers because they can integrate gastric protection, controlled intestinal release, mucoadhesion and surface-charge modulation within one delivery system [6-14].

Alginate and chitosan are particularly suited to oral peptide-delivery design. Alginate forms calcium-crosslinked gels that are comparatively stable under gastric conditions and can swell or relax at intestinal pH. Chitosan is a cationic mucoadhesive polymer that can interact electrostatically with alginate and mucin, producing a polyelectrolyte coating around an alginate core [15-18]. These complementary mechanisms suggest that a chitosan-coated alginate system may shield insulin in the stomach while enabling controlled release and mucosal interaction in intestinal media.

Because nanoparticle performance is sensitive to polymer and crosslinker concentrations, formulation optimization by design of experiments is preferable to one-factor-at-a-time development. Box-Behnken response-surface methodology can estimate linear, interaction and quadratic effects while reducing the number of experimental runs [19-22]. The present manuscript converts the thesis data into a journal-style original research paper focused on the development, optimization and in vitro evaluation of oral insulin-loaded chitosan-coated alginate nanoparticles. The objective was to define an optimized formulation that balances nanoscale size, low PDI, positive zeta potential, high entrapment, low gastric release, controlled intestinal release, enzymatic protection and enhanced in vitro permeation.

II. MATERIALS AND METHODS

2.1 Materials

Human insulin was used as the model peptide. Sodium alginate served as the anionic matrix polymer, chitosan as the cationic coating polymer and calcium chloride dihydrate as the ionic crosslinker. Glacial acetic acid, trehalose, pepsin, pancreatin, phosphate buffer salts and porcine gastric mucin were used for coating, lyophilization, enzymatic challenge, release/permeation media and mucin-interaction experiments. All reagents were analytical grade unless otherwise specified.

2.2 Analytical method and compatibility evaluation

Insulin was estimated by UV-visible spectrophotometry at 276 nm. Working standards were prepared in phosphate buffer pH 7.4 over 2-20 µg/mL. Linearity, precision, accuracy, LOD and LOQ were evaluated according to the general ICH Q2(R2) validation approach. FTIR spectra of insulin, sodium alginate, chitosan, physical mixtures and optimized nanoparticles were recorded from 4000 to 400 cm^-1 to assess preservation of characteristic insulin amide bands and polymer interaction signatures [23-25].

2.3 Preparation of insulin-loaded nanoparticles

Nanoparticles were prepared by aqueous ionic gelation and polyelectrolyte coating. Sodium alginate solution was adjusted to pH 4.5, mixed with insulin equivalent to 100 IU per batch and crosslinked by dropwise addition of calcium chloride under homogenization. The pre-gel dispersion was sonicated to reduce aggregation. Chitosan in 1% v/v acetic acid was adjusted to pH <=5.5 and added dropwise to the alginate-calcium dispersion to form a cationic chitosan coat. The suspension was stirred, centrifuged, washed and lyophilized using 5% w/v trehalose as cryoprotectant.

2.4 Experimental design and optimization

A three-factor, three-level Box-Behnken design was used. Sodium alginate concentration (X1: 1.0, 1.5 and 2.0 mg/mL), chitosan concentration (X2: 0.3, 0.6 and 0.9 mg/mL) and calcium chloride concentration (X3: 10, 20 and 30 mM) were the independent variables. The measured responses were particle size, PDI, zeta potential, entrapment efficiency, process yield, 2 h release in simulated gastric fluid and 8 h release in intestinal media. Quadratic polynomial models were fitted and evaluated by ANOVA, coefficient of determination and lack-of-fit statistics. Numerical desirability was used to select a formulation that minimized PDI and gastric release, targeted particle size near 220 nm and maximized entrapment and controlled intestinal release.

2.5 Nanoparticle characterization

Particle size and PDI were measured by dynamic light scattering after dilution with filtered deionized water. Zeta potential was measured by electrophoretic light scattering. Entrapment efficiency was calculated from the difference between total and free insulin after centrifugation. Drug loading was calculated as entrapped insulin relative to dried nanoparticle mass, and process yield was calculated from dried nanoparticle mass relative to total solid input.

2.6 In vitro release, kinetic modeling and enzymatic stability

In vitro release was studied by dialysis under sequential simulated gastrointestinal conditions: simulated gastric fluid pH 1.2 for 2 h, simulated intestinal fluid pH 6.8 for 6 h and phosphate buffer pH 7.4 up to 12 h. Samples were withdrawn at defined time points and analyzed at 276 nm. Release data for the optimized formulation were fitted to zero-order, first-order, Higuchi and Korsmeyer-Peppas models [26-28]. Enzymatic protection was evaluated by incubating insulin solution and optimized nanoparticles in simulated gastric fluid containing

pepsin, simulated intestinal fluid containing pancreatin and buffer containing trypsin/chymotrypsin. Insulin remaining was expressed relative to initial insulin content.

2.7 Mucin interaction, swelling, permeation and stability

Mucoadhesion was evaluated by mucin-binding, zeta-potential shift after mucin contact, pH-dependent swelling and retention after washing on mucin surfaces. In vitro permeation was evaluated in a diffusion assembly with equivalent insulin concentration in the donor compartment and phosphate buffer pH 7.4 in the receptor compartment. Cumulative permeation was measured at 1, 2, 4, 6 and 8 h, and apparent permeability coefficient was calculated from steady-state flux [29-31]. Stability of the lyophilized optimized batch was examined at 25 ± 2 degC/60 ± 5% RH and 40 ± 2 degC/75 ± 5% RH for 30 days by monitoring particle size, PDI, entrapment efficiency and 8 h release [32].

III. RESULTS

Result datasets are presented as graphs rather than result tables. Mean ± SD is shown where the thesis data reported replicate variability.

3.1 Analytical method, preformulation and compatibility

Insulin absorbance at 276 nm was linear across 2-20 µg/mL using the plotted calibration data (fitted slope 0.0546, intercept 0.0066, R^2 0.9999). Preformulation observations supported the use of an aqueous process: insulin solubility in phosphate buffer pH 7.4 was 1.26 ± 0.04 mg/mL, the insulin stock pH was 7.18 ± 0.05 and drug content was 99.3 ± 1.2%. FTIR peak mapping retained insulin amide I/II/III regions while showing alginate/chitosan complexation in the optimized nanoparticles, supporting physical encapsulation and polyelectrolyte interaction rather than obvious chemical degradation.

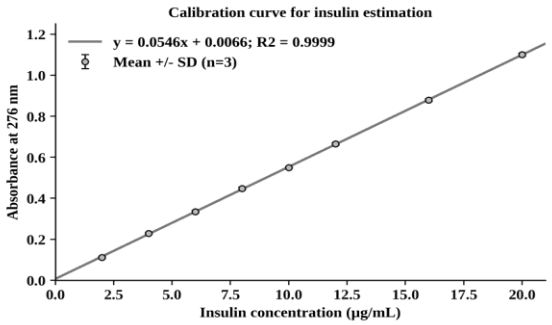

Figure 1. Calibration curve for insulin estimation at 276 nm. Data are mean ± SD (n=3). The plotted linear regression confirms concentration-dependent absorbance across 2-20 µg/mL.

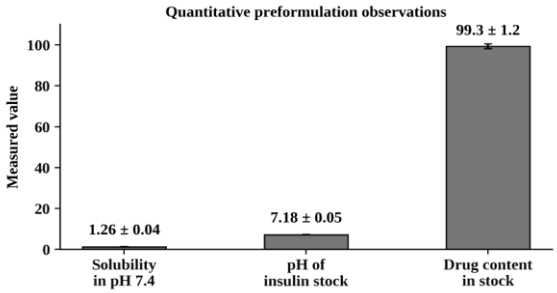

Figure 2. Quantitative preformulation observations used to support aqueous formulation and analysis. Values are shown as mean ± SD where available; units are displayed above bars.

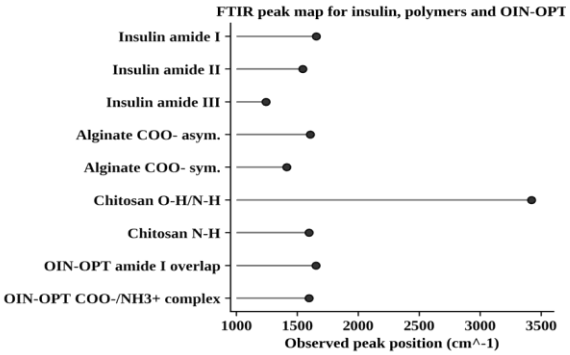

Figure 3. FTIR peak map for insulin, sodium alginate, chitosan and optimized nanoparticles. Retention of the optimized nanoparticle amide I region and shifts in the COO-/NH3+ region are consistent with insulin retention and alginate-chitosan polyelectrolyte interaction.

3.2 Formulation screening and response-surface model adequacy

The 17-run Box-Behnken design produced nanoparticles with particle size from 207.28 to 310.35 nm, PDI from 0.204 to 0.298, zeta potential from

+14.00 to +33.76 mV, entrapment efficiency from 53.53 to 78.89%, process yield from 63.01 to 76.70%, 2 h SGF release from 7.65 to 17.37% and 8 h intestinal release from 51.71 to 73.25%. Higher polymer and crosslinker levels generally increased size and reduced gastric leakage, whereas center-point formulations showed high entrapment and lower PDI. The quadratic models were significant for all critical responses and showed high R^2/adjusted R^2 with non-significant lack-of-fit.

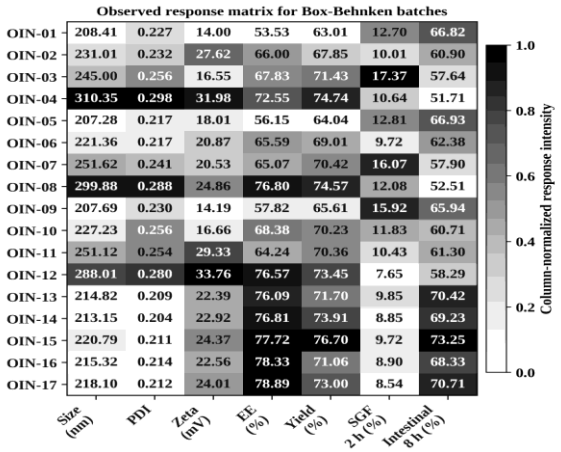

Figure 4. Observed response matrix for the Box-Behnken formulation batches. Values inside cells are raw observed values; color intensity is normalized within each response column to visualize relative response behavior across batches.

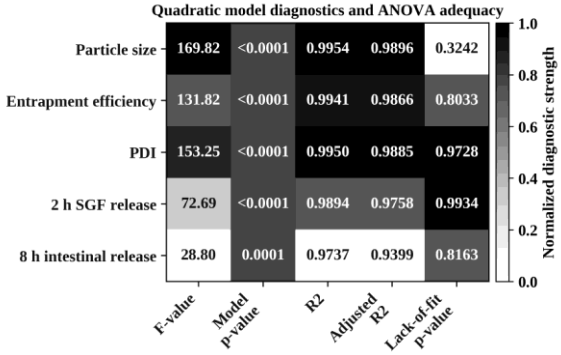

Figure 5. Quadratic model diagnostics. Values inside cells are raw model diagnostics. Model p-values were <0.0001 for particle size, entrapment efficiency, PDI and 2 h SGF release, and 0.0001 for 8 h intestinal release; lack-of-fit p-values were >0.05 for all models, supporting adequacy within the experimental domain.

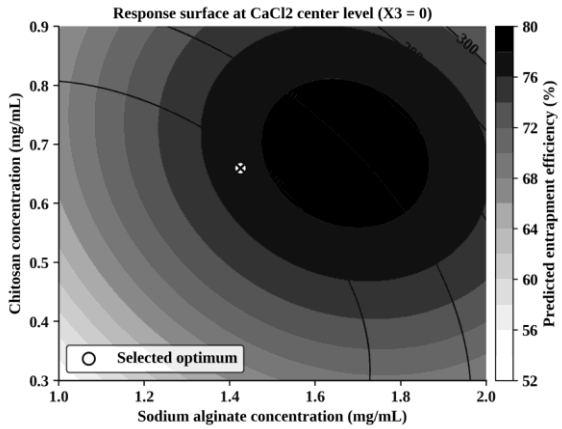

Figure 6. Response surface at the calcium chloride center level (X3 = 0). The filled contours show predicted entrapment efficiency and line contours show predicted particle size. The selected optimum is projected onto the alginate-chitosan plane.

3.3 Optimized formulation and validation

The desirability-selected formulation contained sodium alginate 1.425 mg/mL, chitosan 0.660 mg/mL and calcium chloride 21.5 mM. Validation errors for the five main optimized responses were low: 0.64% for particle size, 0.79% for entrapment efficiency, 0.94% for PDI, 3.57% for 2 h SGF release and 0.62% for 8 h intestinal release. The optimized batch had particle size 221.4 ± 3.7 nm, PDI 0.214 ± 0.011, zeta potential +25.7 ± 1.6 mV, entrapment efficiency 78.6 ± 1.2%, drug loading 7.8 ± 0.3% and process yield 74.8 ± 1.5%.

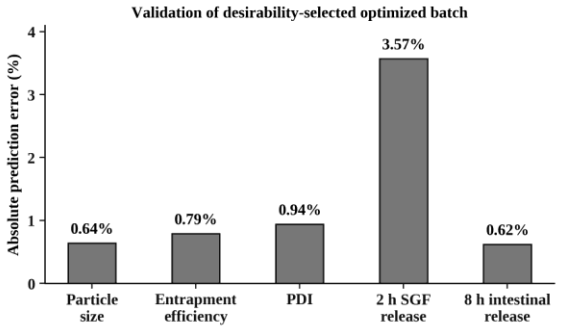

Figure 7. Prediction error for the desirability-selected optimized formulation. The graph shows low deviation between predicted and observed validation responses, with the largest error observed for 2 h gastric release.

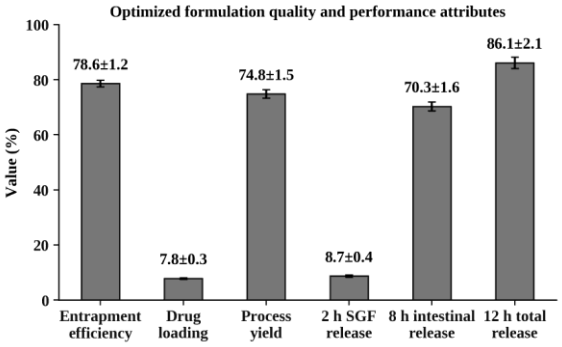

Figure 8. Percent-based quality and performance attributes of optimized nanoparticles. Particle size, PDI and zeta potential were 221.4 ± 3.7 nm, 0.214 ± 0.011 and +25.7 ± 1.6 mV, respectively.

3.4 pH-responsive release and release kinetics

The optimized formulation restricted release under gastric conditions and then released insulin progressively after transfer to intestinal media. At 2 h in simulated gastric fluid, nanoparticle release was 8.7 ± 0.4%, whereas insulin solution had released 97.4 ± 1.5%. Nanoparticles reached 70.3 ± 1.6% release by 8 h and 86.1 ± 2.1% by 12 h. Kinetic fitting gave the highest R^2 for the Korsmeyer-Peppas model (0.9899; n = 1.385), followed by first-order release (R^2 = 0.9851), indicating that pH-triggered swelling, polymer relaxation/erosion and diffusion all contributed to the release mechanism.

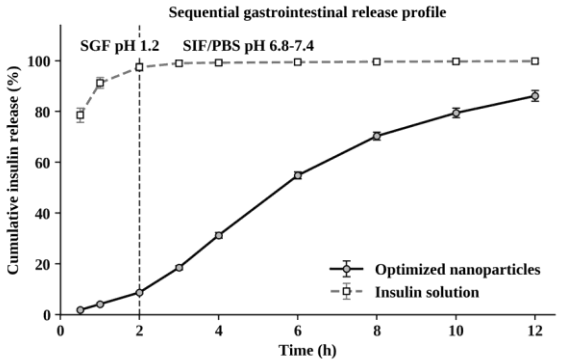

Figure 9. Sequential gastrointestinal release profile of optimized nanoparticles and insulin solution. The dashed line marks transfer after the gastric stage at 2 h. Data are mean ± SD (n=3).

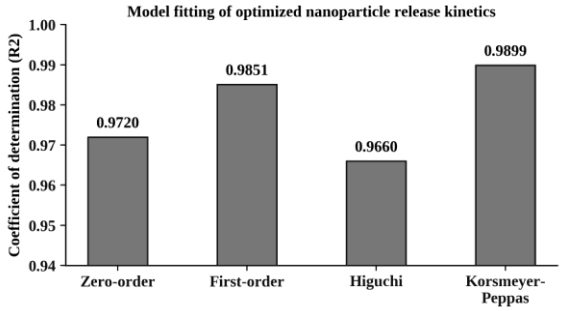

Figure 10. Release kinetic model fitting for optimized nanoparticles. The constants/exponent were k0 = 8.115%/h, k1 = 0.077 h^-1, kH = 34.414% h^-0.5 and Korsmeyer-Peppas n = 1.385.

3.5 Enzymatic protection

The optimized nanoparticles preserved substantially more insulin than solution during enzyme exposure. In simulated gastric fluid containing pepsin, nanoparticles retained 88.9 ± 2.4% insulin at 2 h compared with 28.6 ± 3.1% for insulin solution. Protection was also observed in simulated intestinal fluid containing pancreatin and in trypsin/chymotrypsin buffer, with nanoparticle retention of 79.6 ± 3.1% and 75.8 ± 3.3%, respectively.

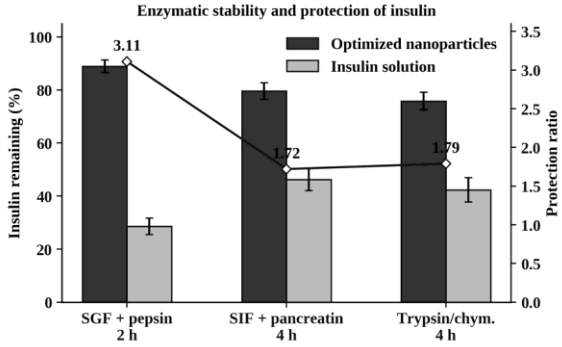

Figure 11. Enzymatic stability and protection of insulin. Bars show insulin remaining after enzyme exposure; protection ratios compare nanoparticle retention with insulin-solution retention.

3.6 Mucoadhesion, mucin interaction and permeation

Mucin binding increased from 8.2 ± 1.1% for insulin solution to 63.8 ± 3.4% for nanoparticles, and mucoadhesive retention after washing increased from 12.4 ± 2.0% to 58.5 ± 3.7%. Swelling was pH-responsive, with 17.4 ± 2.1% swelling in simulated gastric fluid and 68.2 ± 4.8% in simulated intestinal fluid. Mucin contact shifted zeta potential from +25.7

± 1.6 mV to +8.4 ± 1.2 mV, consistent with electrostatic interaction between the chitosan-coated particle surface and mucin.

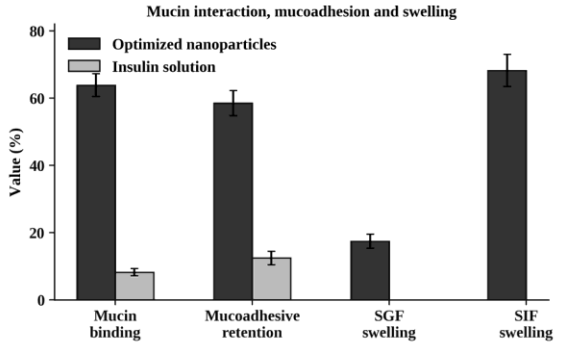

Figure 12. Mucin binding, mucoadhesive retention and pH-responsive swelling. Data are mean ± SD where available; swelling applies to nanoparticles only.

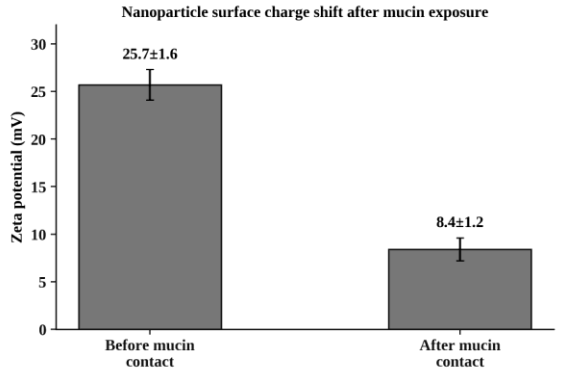

Figure 13. Zeta-potential shift after mucin exposure. Reduced positive surface charge after mucin contact indicates mucin adsorption/interactions on the nanoparticle surface.

Permeation studies showed a consistent nanoparticle advantage. At 8 h, cumulative permeation was 48.6 ± 2.8% for nanoparticles and 19.1 ± 1.4% for insulin solution. The steady-state flux increased from 3.78 ± 0.31 to 9.82 ± 0.54 µg/cm²/h, and apparent permeability coefficient increased from (1.12 ± 0.09) × 10^-6 to (2.91 ± 0.16) × 10^-6 cm/s, corresponding to an enhancement ratio of 2.60. Lag time decreased from 0.95 h for solution to 0.62 h for nanoparticles.

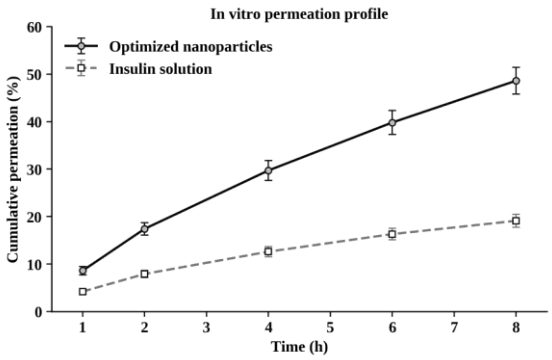

Figure 14. In vitro permeation profile of optimized nanoparticles and insulin solution. Data are mean ± SD (n=3).

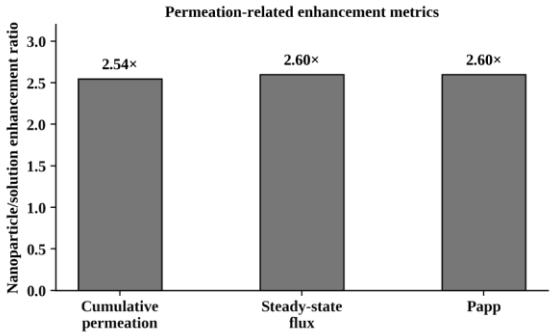

Figure 15. Permeation-related enhancement metrics. Nanoparticle/solution enhancement ratios were 2.54 for cumulative permeation at 8 h, 2.60 for steady-state flux and 2.60 for apparent permeability coefficient.

3.7 Short-term stability

The lyophilized optimized formulation remained comparatively stable for 30 days at 25 ± 2 degC/60 ± 5% RH, with particle size increasing from 221.4 ± 3.7 to 224.9 ± 4.6 nm and entrapment efficiency decreasing from 78.6 ± 1.2% to 76.8 ± 1.6%. Accelerated storage at 40 ± 2 degC/75 ± 5% RH caused a larger increase in particle size and PDI and a greater decrease in entrapment and 8 h release, suggesting that controlled-room-temperature or refrigerated storage with moisture protection should be explored in further development.

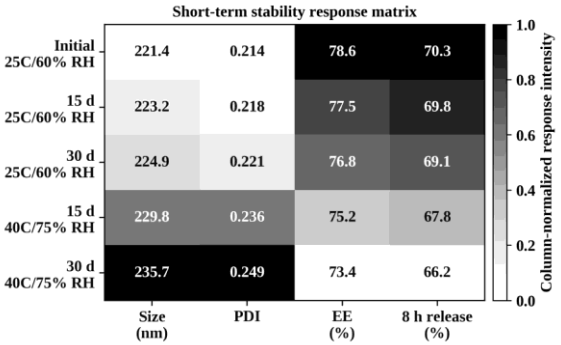

Figure 16. Short-term stability response matrix. Values inside cells are raw stability measurements; color intensity is normalized within each response column to visualize change over storage condition and time.

IV. DISCUSSION

The optimized formulation demonstrates the central design trade-off in oral peptide nanoparticles: sufficient polymer and crosslinking are needed for acid and enzymatic protection, but excessive polymer concentration can increase particle size and dispersity. The response-surface results showed that intermediate formulation space provided the best balance of high entrapment, nanoscale size and controlled release. The positive zeta potential of the optimized batch supports successful chitosan coating, which is expected to promote mucin interaction and retention at absorptive surfaces.

The release profile is consistent with the complementary roles of alginate and chitosan. Calcium alginate can limit matrix hydration and insulin diffusion in acidic medium, whereas intestinal pH favors deprotonation, matrix swelling and relaxation. The observed release behavior and the high Korsmeyer-Peppas fit indicate that more than simple diffusion-controlled insulin liberation; swelling and polymer relaxation/erosion likely contributed to the intestinal release phase.

The enzymatic-stability results are important because peptide degradation is a major barrier to oral insulin delivery. The nanoparticle matrix and coating appear to reduce immediate enzyme contact with insulin, producing the highest protection under the pepsin-containing gastric challenge. The permeation enhancement is also consistent with a multifunctional mechanism: protected insulin release near the diffusion interface, mucoadhesive residence and cationic surface interaction may jointly increase local availability of insulin for transport.

Compared with insulin solution, the optimized nanoparticles achieved substantially lower gastric release, higher enzymatic retention, stronger mucin interaction and higher cumulative permeation. These are encouraging in vitro indicators, but they should not be interpreted as confirmed oral bioavailability. A Q1-level submission would be strengthened by chromatographic confirmation of insulin integrity after formulation and release, bioactivity testing of released insulin, cytotoxicity and transepithelial transport in intestinal cell models, mucus-diffusion studies, in vivo pharmacokinetic/pharmacodynamic evaluation and longer-term stability under final packaging conditions.

A further limitation is that UV absorbance was used for insulin quantification in formulation-development samples. Although the method was linear and validated for the reported matrix conditions, high-impact submissions often benefit from orthogonal HPLC/UPLC confirmation, especially for peptide stability, degradation products and released insulin integrity. Therefore, the present dataset should be positioned as formulation optimization and in vitro proof-of-concept rather than definitive therapeutic validation.

V. CONCLUSION

Chitosan-coated alginate nanoparticles prepared by aqueous ionic gelation provided a balanced oral insulin formulation with nanoscale particle size, narrow PDI, positive surface charge, high insulin entrapment, restricted gastric release, controlled intestinal release, enzymatic protection, strong mucin interaction and improved in vitro permeation compared with insulin solution. The optimized composition was sodium alginate 1.425 mg/mL, chitosan 0.660 mg/mL and calcium chloride 21.5 mM. The findings support this system as a promising in vitro platform for oral insulin-delivery development, while confirming that in vivo bioavailability, pharmacodynamic efficacy, safety and insulin-bioactivity studies are necessary before translational claims can be made.

REFERENCES

[1] Agnihotri SA, Mallikarjuna NN, Aminabhavi TM, "Recent advances on chitosan-based micro- and nanoparticles in drug delivery," *Journal of Controlled Release*, vol. 100, no. 1, pp. 5-28, 2004.

[2] Anselmo AC and Mitragotri S, "Nanoparticles in the clinic: An update," *Bioengineering & Translational Medicine*, vol. 4, no. 3, Art. no. e10143, 2019.

[3] Antosova Z, Mackova M, Kral V, and Macek T, "Therapeutic application of peptides and proteins: Parenteral forever?" *Trends in Biotechnology*, vol. 27, no. 11, pp. 628-635, 2009.

[4] Artursson P, Palm K, and Luthman K, "Caco-2 monolayers in experimental and theoretical predictions of drug transport," *Advanced Drug Delivery Reviews*, vol. 46, nos. 1-3, pp. 27-43, 2001.

[5] Aungst BJ, "Intestinal permeation enhancers," *Journal of Pharmaceutical Sciences*, vol. 89, no. 4, pp. 429-442, 2000.

[6] Barbosa FC, Garcia CS, de Souza Ferreira SB, *et al*., "Progress in the development of chitosan based insulin delivery systems: A systematic review," *Polymers*, vol. 12, no. 11, Art. no. 2499, 2020.

[7] Bernkop-Schnurch A and Dunnhaupt S, "Chitosan-based drug delivery systems," *European Journal of Pharmaceutics and Biopharmaceutics*, vol. 81, no. 3, pp. 463-469, 2012.

[8] Bhattacharjee S, "DLS and zeta potential: What they are and what they are not?" *Journal of Controlled Release*, vol. 235, pp. 337-351, 2016.

[9] Box GEP and Behnken DW, "Some new three level designs for the study of quantitative variables," *Technometrics*, vol. 2, no. 4, pp. 455-475, 1960.

[10] Bruno BJ, Miller GD, and Lim CS, "Basics and recent advances in peptide and protein drug delivery," *Therapeutic Delivery*, vol. 4, no. 11, pp. 1443-1467, 2013.

[11] Calvo P, Remunan-Lopez C, Vila-Jato JL, and Alonso MJ, "Novel hydrophilic chitosan-polyethylene oxide nanoparticles as protein carriers," *Journal of Applied Polymer Science*, vol. 63, no. 1, pp. 125-132, 1997.

[12] des Rieux A, Fievez V, Garinot M, Schneider YJ, and Preat V, "Nanoparticles as potential oral delivery systems of proteins and vaccines: A mechanistic approach," *Journal of Controlled Release*, vol. 116, no. 1, pp. 1-27, 2006.

[13] Ensign LM, Cone R, and Hanes J, "Oral drug delivery with polymeric nanoparticles: The gastrointestinal mucus barriers," *Advanced Drug Delivery Reviews*, vol. 64, no. 6, pp. 557-570, 2012.

[14] Fonte P, Araujo F, Reis S, and Sarmento B, "Oral insulin delivery: How far are we?" *Journal of Diabetes Science and Technology*, vol. 7, no. 2, pp. 520-531, 2013.

[15] George M and Abraham TE, "Polyionic hydrocolloids for the intestinal delivery of protein drugs: Alginate and chitosan," *Journal of Controlled Release*, vol. 114, no. 1, pp. 1-14, 2006.

[16] Gedawy A, Martinez J, Al-Salami H, and Dass CR, "Oral insulin delivery: Existing barriers and current counter-strategies," *Journal of Pharmacy and Pharmacology*, vol. 70, no. 2, pp. 197-213, 2018.

[17] He Z, Santos JL, Tian H, *et al*., "Scalable fabrication of size-controlled chitosan nanoparticles for oral delivery of insulin," *Biomaterials*, vol. 130, pp. 28-41, 2017.

[18] Higuchi T, "Mechanism of sustained-action medication: Theoretical analysis of rate of release of solid drugs dispersed in solid matrices," *Journal of Pharmaceutical Sciences*, vol. 52, no. 12, pp. 1145-1149, 1963.

[19] International Council for Harmonisation, *ICH Q2(R2): Validation of Analytical Procedures*. Geneva, Switzerland: ICH, 2023.

[20] International Council for Harmonisation, *ICH Q1A(R2): Stability Testing of New Drug Substances and Products*. Geneva, Switzerland: ICH, 2003.

[21] International Diabetes Federation, *IDF Diabetes Atlas*, 11th ed. Brussels, Belgium: International Diabetes Federation, 2025.

[22] Jaafar MHM and Hamid KA, "Chitosan-coated alginate nanoparticles enhanced absorption profile of insulin via oral administration,"

Current Drug Delivery, vol. 16, no. 7, pp. 672-686, 2019.

[23] Korsmeyer RW, Gurny R, Doelker E, Buri P, and Peppas NA, "Mechanisms of solute release from porous hydrophilic polymers," *International Journal of Pharmaceutics*, vol. 15, no. 1, pp. 25-35, 1983.

[24] Lee KY and Mooney DJ, "Alginate: Properties and biomedical applications," *Progress in Polymer Science*, vol. 37, no. 1, pp. 106-126, 2012.

[25] Li X, Qi J, Xie Y, *et al*., "Nanoemulsions coated with alginate/chitosan as oral insulin delivery systems: Preparation, characterization, and hypoglycemic effect in rats," *International Journal of Nanomedicine*, vol. 8, pp. 23-32, 2013.

[26] Lopes M, Shrestha N, Correia A, *et al*., "Dual chitosan/albumin-coated alginate/dextran sulfate nanoparticles for enhanced oral delivery of insulin," *Journal of Controlled Release*, vol. 232, pp. 29-41, 2016.

[27] Mahato RI, Narang AS, Thoma L, and Miller DD, "Emerging trends in oral delivery of peptide and protein drugs," *Critical Reviews in Therapeutic Drug Carrier Systems*, vol. 20, nos. 2-3, pp. 153-214, 2003.

[28] Montgomery DC, *Design and Analysis of Experiments*, 10th ed. Hoboken, NJ, USA: Wiley, 2019.

[29] Pessoa B, Correia A, Andrade F, *et al*., "Chitosan/albumin coating factorial optimization of alginate/dextran sulfate nanoparticles for oral insulin delivery," *Marine Drugs*, vol. 21, no. 3, Art. no. 165, 2023.

[30] Ritger PL and Peppas NA, "A simple equation for description of solute release II: Fickian and anomalous release from swellable devices," *Journal of Controlled Release*, vol. 5, no. 1, pp. 37-42, 1987.

[31] Sarmento B, Ribeiro A, Veiga F, Sampaio P, Neufeld R, and Ferreira D, "Alginate/chitosan nanoparticles are effective for oral insulin delivery," *Pharmaceutical Research*, vol. 24, no. 12, pp. 2198-2206, 2007.

[32] Seyam S, Nordin NA, and Alfatama M, "Recent progress of chitosan and chitosan derivatives-based nanoparticles: Pharmaceutical perspectives of oral insulin delivery," *Pharmaceuticals*, vol. 13, no. 10, Art. no. 307, 2020.

[33] Thanou M, Verhoef JC, and Junginger HE, "Oral drug absorption enhancement by chitosan and its derivatives," *Advanced Drug Delivery Reviews*, vol. 52, no. 2, pp. 117-126, 2001.

[34] Vila A, Sanchez A, Tobio M, Calvo P, and Alonso MJ, "Design of biodegradable particles for protein delivery," *Journal of Controlled Release*, vol. 78, nos. 1-3, pp. 15-24, 2002.

[35] Wang Y, Li H, Rasool A, Wang H, Manzoor R, and Zhang G, "Polymeric nanoparticles for oral delivery of insulin," *Journal of Nanobiotechnology*, vol. 22, Art. no. 1, 2024.

[36] Woitiski CB, Veiga F, Ribeiro A, and Neufeld R, "Design for optimization of nanoparticles integrating biomaterials for orally dosed insulin," *European Journal of Pharmaceutics and Biopharmaceutics*, vol. 73, no. 1, pp. 25-33, 2009.

[37] Wong CY, Al-Salami H, and Dass CR, "Potential of insulin nanoparticle formulations for oral delivery and diabetes treatment," *Journal of Controlled Release*, vol. 264, pp. 247-275, 2017.

[38] Zhang E, Zhu H, Song B, Shi Y, and Cao Z, "Recent advances in oral insulin delivery technologies," *Journal of Controlled Release*, vol. 366, pp. 221-230, 2024.